On the antenna calibration of space radio instruments using the galactic background: General formulas and application to STEREO/WAVES

A. Zaslavsky,[1] N. Meyer-Vernet,[1] S. Hoang,[1] M. Maksimovic,[1] and S. D. Bale[2]

[1]   We present general formulas to calibrate the antennas of a space-based radio instrument using as a reference source the galactic background radiation (or any isotropic source). We apply these formulas to determine the effective length of the STEREO/ WAVES antennas. The results for the monopoles are in agreement with the measurements performed on ground, and we provide new results for the XY and YZ dipoles used by the instrument. Our method also allows us to accurately determine the internal noise background of the radio receiver.

1.   Introduction

[2]   Radio receivers onboard spacecraft measure electromagnetic radiation via the fluctuating electric potential at the terminals of electric antennas. The signal is converted through a spectral analysis performed onboard into a voltage power spectral density V_f^2 which is telemetered back to Earth. To enable a comparison of the measurement performed by different antenna systems, it is thus necessary to convert this power spectral density into a physical quantity characterizing the radiation itself. This quantity can be the brightness B_f of the source, or the electromagnetic flux density S_f incoming on the antennas.

[3]   A classical method to perform this calibration is to observe a known source of electromagnetic radiation, and to relate the measured V_f^2 to the modeled flux of the source. A convenient source for this purpose is the radio background radiation of the galaxy, for several reasons. First, it is relatively constant in time and widely measured [*Cane*, 1979; *Novacco and Brown*, 1978]. Second, it is the dominant emission (in the absence of strong solar or planetary sporadic emissions) in the frequency range 500 kHz to 10 MHz; and third, the source covers a 4π solid angle roughly isotropically (modulations as a function of the observed solid angle are less than 20% in the considered frequency range [*Manning and Dulk*, 2001], and will be neglected here), which makes the calibration process easier: it does not rely on the antenna orientation in space, and one can use basic thermodynamic relations between the antenna and the source temperatures.

[4]   In section 2, we present the general relations between the signal measured by the radio receiver and the incoming electromagnetic flux density (or equivalently, the observed source brightness). In section 3, we apply these relations to the antenna calibration of the STEREO/WAVES (S/WAVES) radio instrument onboard the STEREO spacecraft [*Bougeret et al.*, 2008] using the galactic radio background as a reference source. This enables us to perform an in-flight measurement of the effective length of the various monopoles (measuring the potential difference between an antenna and the spacecraft body) and dipoles (measuring the potential difference between two antennas) used by the instrument [*Bale et al.*, 2008].

2.   Calibration Formulas for a Dipole Antenna

[5]   In this section, we present the relation between the voltage power spectral density at an antenna terminals and the incident electromagnetic flux. We first derive a general result based on the thermodynamic properties of the antenna-radiation equilibrium, valid for any antenna geometry. The assumption is that the source brightness is constant over the beam area of the antenna (which is of course the case for an isotropic source).

[1]Laboratoire d'Etudes Spatiales et d'Instrumentation en Astrophysique, Observatoire de Paris-CNRS-Université Pierre et Marie Curie-Université Denis Diderot, Meudon, France.
[2]Space Sciences Laboratory, University of California, Berkeley, California, USA.

2.1. Basic Formulas

[6] A lossless antenna can be modeled by a complex impedance, whose real part is usually called its radiation resistance R_r, which depends both on the geometrical properties of the antenna and on the frequency f considered.

[7] To derive a general calibration formula, we consider an antenna in thermal equilibrium with the surrounding electromagnetic radiation. In open circuit situation (i.e., the antenna is connected to a receiver of infinite impedance), the voltage power spectral density V_f^2 at the terminals of the antenna is related to the temperature T of both the antenna and the radiation by Nyquist's [1928] formula

$$V_f^2 = 4k_B T R_r, \qquad (1)$$

where k_B is Boltzmann's constant. V_f^2 is the Fourier transform of the autocorrelation function of the fluctuating electric potential $V(t)$ at the antenna terminals, so that

$$V_f^2 = 2 \int_{-\infty}^{+\infty} <V(t)V(t+\tau)> e^{i2\pi f \tau} d\tau, \qquad (2)$$

where the brackets denote time averaging, the usual convention of positive frequencies is implied, and V_f^2 is in units V^2/Hz.

[8] The temperature T of the electromagnetic source is related to its brightness B_f (in units $W/m^2/Hz/sr$) at a given wavelength $\lambda = c/f$ by the Rayleigh-Jeans law

$$B_f = 2\frac{k_B T}{\lambda^2}, \qquad (3)$$

so that we can directly relate the voltage at the antenna terminals to the brightness of the source

$$V_f^2 = 2R_r \lambda^2 B_f. \qquad (4)$$

[9] Note that the electromagnetic flux density S_f from the source is related to its brightness by the relation $S_f = B_f \Omega_S$ where the source solid angle Ω_S is 4π for the presently considered isotropic case.

2.2. Voltage Measured by the Space Radio Receiver

[10] In space, the antenna is electrically connected to a large input impedance receiver through the deployment mechanism (the antenna base) and various connection cables, the impedance of which must be taken into account [Manning, 2000]. The latter is commonly called stray (or base) impedance Z_s. The effective voltage power spectral density V_r^2 measured by the receiver is thus

$$V_r^2 = \left| \frac{Z_s}{Z_a + Z_s} \right|^2 V_f^2 \equiv \Gamma^2 V_f^2, \qquad (5)$$

where Z_a and Z_s are the antenna impedance and the stray impedance determined by the spacecraft design, respectively. Since in the radio frequency range (at frequencies well above the kHz), the resistive part of these impedances is negligible (typically, at 1 MHz, $1/\omega C_{a,s} \sim 10\ k\Omega$ whereas $R_r \sim 1\ \Omega$), the gain factor reduces to $\Gamma = C_a/(C_a + C_s)$, where C_a and C_s are the antenna and the stray capacitances, respectively. This shows the importance of minimizing the stray capacitance to increase the radio receivers sensitivity.

[11] Two other contributions to the power spectrum must be taken into account. The first one is the noise produced by the receiver itself. All the electronic components in the receiver produce a fluctuating noise, which can be represented by a current source I_{noise} characteristic of the receiver. When connected to a device of given impedance Z, like an antenna, it generates a noise square voltage $V_{noise}^2 = |Z I_{noise}|^2$ which is superimposed to the external signal. It is important to note that this noise depends both on the receiver and on the impedance connected to it.

[12] The second contribution is the quasi-thermal noise produced by the ambient plasma, which strongly perturbs the galactic background measurements at low frequencies [Meyer-Vernet et al., 2000]. It is given at frequencies $f \gg f_p L_D/L$, where f_p and L_D are the local plasma frequency and Debye length, by [Meyer-Vernet and Perche, 1989]

$$V_{QTN}^2 \simeq 5.10^{-5} \frac{n_e T_e}{f^3 L}, \qquad (6)$$

where n_e and T_e are the local electron density (cm^{-3}) and temperature (K), f is the considered frequency (Hz) and L the physical length (m) of one boom (or arm) of the dipole. Equation (6) gives the noise induced at the terminals of the antenna, and is therefore related to the noise detected by the receiver by the factor Γ^2.

[13] Thus, the relation between the brightness of the source and the voltage power spectral density at the output of the receiver is

$$V_r^2 = V_{noise}^2 + \Gamma^2 V_{QTN}^2 + 2\Gamma^2 R_r \lambda^2 B_f, \quad \Gamma = \frac{C_a}{C_a + C_s}. \qquad (7)$$

2.3. Short Dipole

[14] The simplest case to consider, and the most useful for space radioastronomy, is that of a short dipole. The short dipole approximation is valid as long as the wavelength λ is much larger than the physical dimensions of the antenna. In this case, the radiation resistance is given by, e.g., [Kraus and Marhefka, 2003]

$$R_r = \frac{2\pi}{3} Z_0 \left(\frac{l_{eff}}{\lambda} \right)^2, \qquad (8)$$

where $Z_0 = \sqrt{\mu_0/\epsilon_0} \simeq 120\pi$ is the impedance of vacuum, and l_{eff} the effective length (also called electrical length) of the dipole, characterizing its electrical response. The effective length of an antenna is defined by

$$l_{eff} = \frac{V}{E}, \qquad (9)$$

where V is the voltage induced at the antenna terminals by an incoming electromagnetic plane wave of electric field E, when the electric field direction is parallel to the direction of the antenna [*Kraus and Marhefka*, 2003; *Schelkunoff and Friis*, 1952].

[15] The voltage V is related to E through the current distribution in the antenna by the relation

$$V = \frac{1}{I_0} \int_{antenna} E(z)I(z)dz. \qquad (10)$$

In the case of a short dipole, $E(z)$ can be put outside the integral, and l_{eff} is thus equal to the integral of the current distribution $I(z)$ induced in the antenna divided by I_0.

[16] The effective length l_{eff} of the dipole thus strongly depends on the current distribution in the antenna. In the ideal case of a short dipole antenna made of two aligned wires, each of length L, the derivation of the effective length from (10) is straightforward and yields $l_{eff} = L$. Nevertheless, for most space applications, as we shall see in section 3, the actual shape of the antennas as well as the presence of electrical currents in the conductive body of the spacecraft can produce important deviations from this ideal picture.

[17] Introducing (8) into (7), one obtains the relation between the receiver voltage power spectral density and the source brightness in the short dipole regime

$$V_r^2 = V_{noise}^2 + \Gamma^2 V_{QTN}^2 + \frac{4\pi}{3} Z_0 \Gamma^2 l_{eff}^2 B_f. \qquad (11)$$

We show in the appendix that the same result is found by calculating the voltage generated in a short dipole antenna by incident unpolarized waves coming from all directions.

[18] Note that equation (11) differs by a factor of 2 from the relation between V_r and the source brightness used by *Zarka et al.* [2004] for the calibration of Cassini radio measurements. This has no influence on the flux calibration provided in their paper, which is independent of any constant factor (but leads to overestimated stray capacitances in their section 3).

[19] *Eastwood et al.* [2009] used the expression from *Zarka et al.* [2004] to calibrate the S/WAVES instrument, and on the other hand derived an erroneous relation $l_{eff} = \sqrt{2/3}L$ for a short dipole in free space.

[20] *Hillan et al.* [2010] in their recent work on the Wind WAVES instrument, both used the inadequate l_{eff}

expression derived by *Eastwood et al.* [2009] and an expression linking V_r to the source brightness differing from (11) by a factor of 2/3.

3. Antenna Calibration of the S/WAVES Instrument Onboard STEREO

[21] In this section, we apply the formulas presented above to derive the effective length of the S/WAVES antennas [*Bale et al.*, 2008], using the isotropic galactic background radiation as a calibration source. We shall use equation (11) to compare the minimum background measured by the receiver with a galactic radiation model in a frequency range where the short dipole hypothesis is valid.

3.1. Galactic Background

[22] The galactic background was observed on 13 January 2007. On this day, all the monopole and dipole modes of both STEREO A and B were working on the whole 100 kHz to 16 MHz range of the HF receiver. For each antenna configuration on each spacecraft and at each observing frequency, we consider the total background received (in V^2/Hz) to be the lowest 1% of the data observed within the day.

[23] Then we compared this minimum background to a sky radio background model. In the frequency range considered, two models are mainly used: the *Novacco and Brown* [1978] model and the *Cane* [1979] model. Both are empirical models for the isotropic sky background brightness, based on space measurements (and ground measurements for the high-frequency part of the *Cane* [1979] model). For our calibration, we use the *Novacco and Brown* [1978] model expressed by

$$B_{model} = B_0 f_{MHz}^{-0.76} e^{-\tau}, \qquad (12)$$

where f_{MHz} is the frequency expressed in MHz, $\tau = 3.28 f_{MHz}^{-0.64}$, $B_0 = 1.38 \times 10^{-19}$ $W/m^2/Hz/sr$. The reason for this choice is that this model fitted our data better than the *Cane* [1979] model, as will be explained in section 3.3.

3.2. Determination of Γl_{eff}

[24] Calculating the ratio $(V_r^2 - V_{noise}^2 - \Gamma^2 V_{QTN}^2)/B_{model}$, we obtain from equation (7) a calibration function equal to $2R_r\Gamma^2\lambda^2$. In the short dipole approximation (i.e., $L \ll \lambda$), equation (7) reduces to equation (11), which yields

$$\Gamma l_{eff} = \left(\frac{3}{4\pi Z_0} \frac{V_r^2 - V_{noise}^2 - \Gamma^2 V_{QTN}^2}{B_{model}} \right)^{1/2}. \qquad (13)$$

Therefore our calibration method yields the Γl_{eff} product, which can be considered to be a "reduced effective length". This quantity should not depend on the frequency, since
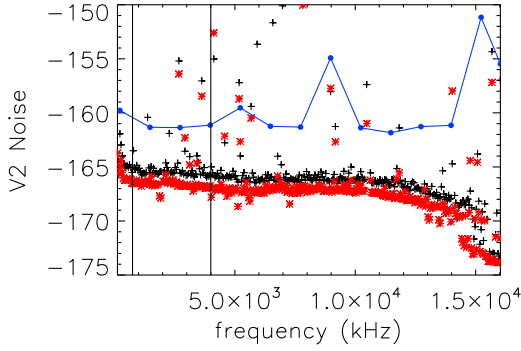
Figure 1. Measurements of the voltage spectral density (in dB) of the STEREO B high-frequency receiver (channel 1) performed to evaluate the receiver internal noise. Blue solid line with circles is the noise before the deployment of the antennas. Black crosses are from the ground test (NASA, Goddard Space Flight Center). Red asterisks are from the ground test (Observatoire de Paris, LESIA). The frequency interval in which the analysis is performed is delimited by the two vertical lines.

neither the effective length nor the antenna capacitance of the short dipole does in the frequency range where the short dipole approximation holds. Thus we determine Γl_{eff} by taking the average of the right-hand side of equation (13) in a frequency range where it is found to be a constant.

[25] One must note that the evaluation of V_{QTN}^2 is complicated as it depends on the local plasma parameters. We thus chose not to include the $-\Gamma^2 V_{QTN}^2$ term in equation (13), and perform the analysis in a frequency interval where this term is negligible.

[26] We have chosen empirically the frequency range 750 kHz to 4 MHz to perform our analysis, for all the antenna configurations. Above 4 MHz the short dipole approximation does not hold, whereas below 750 kHz, the plasma thermal noise is not negligible.

[27] Since the sky background signal detected by S/WAVES is not much above the receiver noise (as can be seen from Figures 1 and 3), we must know the V_{noise}^2 level as accurately as possible to perform the calibration. Figure 1 shows the power spectral density detected by the receiver on STEREO B for different situations: in-flight before the deployment of the antennas (higher curve) and for different tests performed on ground (where the receiver was connected to a 50 Ω resistance). The latter tests provide a lower limit for the receiver noise, as the antenna impedances are much larger than 50 Ω. Figure 1 shows that there exists a difference of 5–6 dB (here and in the following, the dB scale is relative to 1 V^2/Hz) between the higher and the lower curves, with no possibility to determine precisely the level of the actual noise (which has been observed to vary slightly with time (V. Krupar, private communication, 2010)).

[28] Thus, in order to obtain an accurate value of Γl_{eff}, we varied the parameter V_{noise}^2 between the extreme values −166 and −160 dB (we considered the noise to be frequency independent, which is nearly the case in the considered frequency range). For each value of V_{noise}^2 we calculate the mean of the function (13) in the interval 0.75–4 MHz, as well as the χ^2 of the data points with respect to this mean, and retain the values V_{noise}^2 and Γl_{eff} minimizing this χ^2, the uncertainty on Γl_{eff} being defined as $\sqrt{\chi^2/N_{data}}$. Figure 2 shows an example of such a fit, in the case of the XY dipole on STEREO B.

3.3. Determination of the Effective Length

[29] In order to deduce the effective lengths of the dipoles and monopoles on the STEREO spacecraft, we have to model the gain function Γ. Equation (7) shows that we need to know the antenna capacitance C_a and the stray capacitance C_s. The first one can be estimated analytically assuming that the antennas are cylindrical, of length L per boom and radius a [Schelkunoff and Friis, 1952]

$$C_a = \frac{\epsilon_0 \pi}{k} \frac{\tan(kL)}{\log(L/a) - 1}. \qquad (14)$$

[30] We use this formula, replacing L by half the length of the physical dipole (between the tip of the antennas, that is $2L = 10.4$ m for STEREO), and taking for a
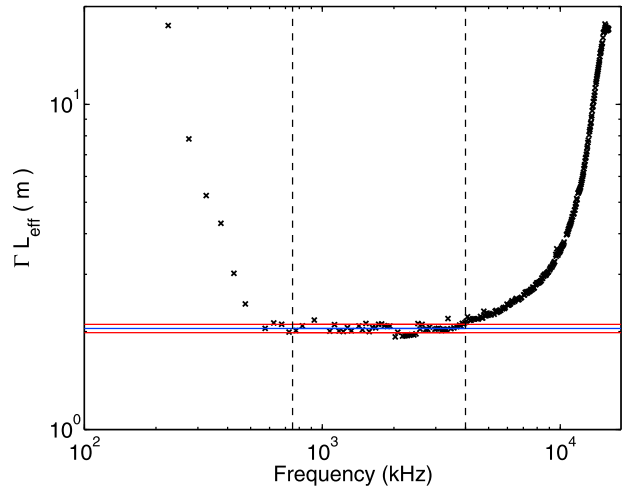

Figure 2. Right-hand side of equation (13) as a function of the frequency. The horizontal lines show the mean value Γl_{eff} (and 1σ uncertainties) calculated in the frequency range between the two dashed vertical lines for the minimum χ^2 fit (yielding $V_{noise}^2 = -162.4$ dB). The measurements are made by the XY dipole on STEREO B on 13 January 2007.

Table 1. Results of the Calibration[a]

Spacecraft	Antenna Configuration	V_{noise}^2 (dB)	Γl_{eff} (m)	l_{eff} (m)
STEREO A	XY Dipole	−160.9	2.02 ± 0.074	4.25 ± 0.15
STEREO A	Z Monopole	−162.8	1.19 ± 0.15	2.35 ± 0.30
STEREO A	X Monopole	−161.8	1.40 ± 0.079	2.77 ± 0.16
STEREO A	YZ Dipole	−161.6	2.06 ± 0.12	4.32 ± 0.27
STEREO B	XY Dipole	−162.4	2.04 ± 0.060	4.30 ± 0.12
STEREO B	Z Monopole	−165.9	1.08 ± 0.10	2.13 ± 0.20
STEREO B	X Monopole	−163.2	1.51 ± 0.073	2.98 ± 0.16
STEREO B	YZ Dipole	−164.2	1.85 ± 0.15	3.89 ± 0.15

[a]Measurements performed on 13 January 2007.

the average radius of the conical antennas of STEREO: $a = 1.15$ cm. The monopole case can be roughly modeled as the one of an antenna on an "infinite ground plane": we must then take for L the physical length of the boom (that is $L = 6$ m on STEREO), and multiply the right side of equation (14) by 2.

[31] The second point is to know the stray capacitance: this one has been measured on ground [*Bale et al.*, 2008] as well as in flight [*Zouganelis et al.*, 2010], giving the same value of $C_s \simeq 32$ *pF* for the dipole mode. The stray capacitance for the monopoles is twice this value, as the dipole is composed of two monopoles electrically associated in series.

[32] Finally, using the measured value $C_s \simeq 32$ *pF* and equation (14) for C_a, we are able to derive the values of l_{eff} from the Γl_{eff} previously obtained. All the results of the fits are presented in Table 1. Figure 3 shows the comparison of the signal $V_r^2 - V_{noise}^2$ with a theoretical prediction based on the *Novacco and Brown* [1978] model (12) and the formula (11) in which the l_{eff} and V_{noise}^2 parameters are given by the minimum χ^2 fit. Figure 3 shows a good agreement between the data and the model in the short dipole frequency range: between 750 kHz and 4 MHz, the relative error between the data and the model curve is less than 5%. Performing a similar study using the *Cane* [1979] galactic background model as a calibration reference provides a lesser agreement, with relative errors of the order of 10%, justifying the use of the *Novacco and Brown* [1978] model for our calibration. For illustration and comparison, Figure 4 shows the two models of galactic background together with the received background data as functions of frequency.

[33] At low frequencies, the dominant signal is not the sky background, but the plasma thermal noise given by equation (6). For typical solar wind parameters at 1 AU, $n_e = 5$ cm^{-3} and $T_e = 10^5$ K, this noise is stronger than the sky background below $f \simeq 500$ kHz, as can be seen in Figure 3. Note that at these high frequencies, the plasma shot noise is negligible, since it decreases as f^{-4} for $f \gg f_p$.

[34] At higher frequencies, the half-wave antenna resonance modifies the expression of the effective length,

which now depends on the frequency. This effect is not taken into account here, which explains why the receiver power spectral density increases faster in the data than in the model. Indeed, the increase observed in the model curve is due to the electrical resonance (increase of Γ when the antenna becomes inductive and $C_a \rightarrow -C_s$), whereas the increase in the data curve is due to both the electrical circuit resonance and the half-wave antenna resonance.

3.4. Calibration Results

[35] Table 1 presents the results of the calibration technique presented above, for all the antenna configurations on both STEREO A and B. The results presented here are in agreement with the rheometry measurements and with antenna modeling [*Bale et al.*, 2008; *Macher et al.*, 2007] for the X and Z monopoles. The effective lengths of the XY and YZ dipoles had not been measured previously.

[36] The receiver noise level has never been measured in space, where the receiver is actually embedded in the solar wind plasma. Table 1 thus also provides the first
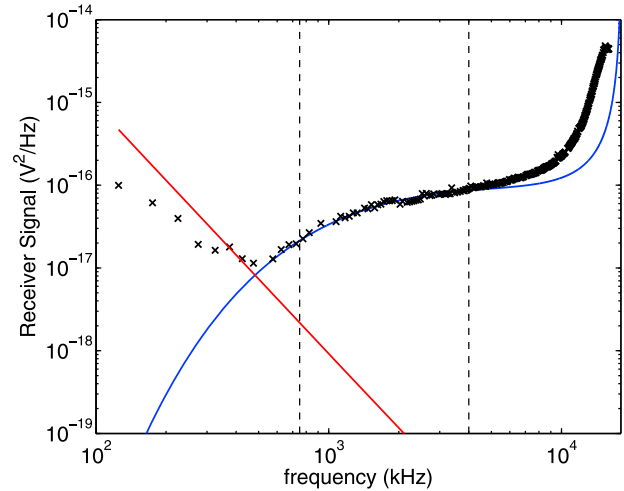

Figure 3. Receiver power spectral density $V_r^2 - V_{noise}^2$ as a function of the frequency. The black crosses are the data points obtained for the dipole XY on STEREO B. The blue solid line is the theoretical receiver power calculated from equations (11), (12), and (14). The effective length is $l_{eff} = 4.30$ m and the noise level is $V_{noise}^2 = -162.4$ dB. The red line is an approximation of the thermal plasma noise $\Gamma^2 V_{QTN}^2$, calculated from equation (6) with typical solar wind parameters $n_e = 5$ cm^{-3} and $T_e = 10^5$ K. The increase of the measured voltage spectral power at frequencies above 4 MHz (at the right of the dashed line) is the consequence of the antenna resonance discussed in the text.
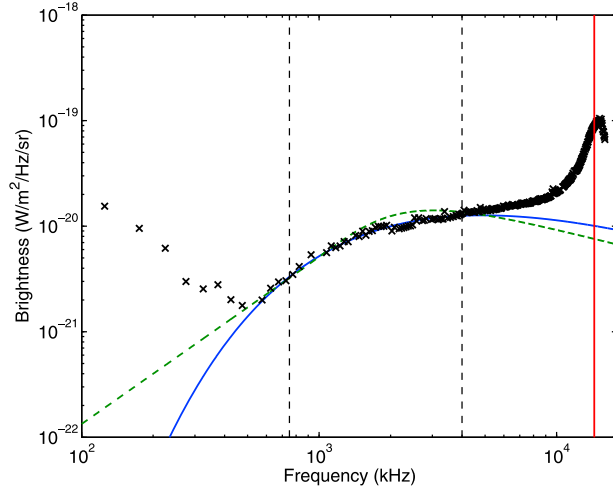
Figure 4. Calibrated data expressed in terms of brightness as a function of the frequency (black crosses). The galactic background radiation models from *Novacco and Brown* [1978] (blue solid line) and *Cane* [1979] (green dashed line) are over plotted. The red line shows the frequency of the theoretical half-wave resonance frequency. The points corresponding to frequencies below $f \sim 500$ kHz are due to the plasma thermal noise detection by the antenna and thus should not be understood in terms of brightness.

measurements of the receiver internal noise level in flight. It must be noted that small variations (±0.5 dB) of this noise can happen, due to slight changes of either the temperature or the voltage delivered by the power supply inside the S/WAVES electronic box (P.-L. Astier, private communication, 2010).

[37] Figure 4 presents the calibrated galactic background brightness as a function of the frequency, and its comparison with galactic background models from the *Novacco and Brown* [1978] and *Cane* [1979] models.

4. Conclusion

[38] We have presented simple formulas to calibrate the antennas of a space-based radio instrument using the isotropic nonthermal galactic radio background. Despite their simplicity, these formulas do not appear to be well known, as inadequate formulas are still used in the literature.

[39] We have applied these formulas to the calibration of the S/WAVES instrument. This enabled us to perform the first in-flight measurements of the effective lengths of the electrical monopoles and dipoles used in the experiment, as well as the accurate determination of the HF Receiver noise level for each antenna configuration and each spacecraft.

[40] Let us finally note that our technique provides accurate values of the reduced effective length Γl_{eff}, but that the values obtained for l_{eff} rely on the gain Γ, which depends on independent measurements of the antenna and stray capacitances.

Appendix A: Direct Calculation of the Voltage Power Spectral Density Measured by a Short Electric Dipole Antenna

[41] The square of the voltage fluctuations of frequency f induced on a short dipole antenna of effective length l_{eff} by an electric field E_f coming from a direction defined by the infinitesimal solid angle $d\Omega$ is, by definition of the effective length (9),

$$d\left(V_f^2\right) = \frac{1}{2}l_{eff}^2 E_f^2(\Omega)\sin^2\theta d\Omega, \tag{A1}$$

where the 1/2 factor comes from the averaging over all the possible linear polarizations (we consider an unpolarized source). The angle θ is defined as the angle between the wave vector k and the linear antenna direction. The effective voltage fluctuations can thus be obtained by integrating (A1) over the solid angle Ω_S occupied by the source

$$V_f^2 = \frac{l_{eff}^2}{2}\int_{\Omega_S} E_f^2(\Omega)\sin^3\theta d\theta d\phi. \tag{A2}$$

[42] Here $E_f^2(\Omega)$ has the dimension of an angular density of square electric field fluctuations per frequency, and is simply related to the brightness of the source by $B_f(\Omega) = E_f^2(\Omega)/Z_0$.

[43] Considering the galaxy as an homogeneous source (i.e., B_f does not depend on Ω) extending over $\Omega_S = 4\pi$, equation (A2) can be immediately integrated to yield

$$V_f^2 = \frac{4\pi}{3}Z_0 l_{eff}^2 B_f, \tag{A3}$$

multiplying by the gain factor Γ^2 and adding the receiver and thermal noises, one finds (11) for V_r^2.

References

Bale, S., et al. (2008), The electric antennas for the STEREO/WAVES experiment, *Space Sci. Rev.*, *136*, 529–547.

Bougeret, J., et al. (2008), S/WAVES: The radio and plasma wave investigation on the stereo mission, *Space Sci. Rev.*, *136*, 487–528.

Cane, H. (1979), Spectra of the non-thermal radio radiation from the galactic polar regions, *Mon. Not. R. Astron. Soc*, *189*, 465–478.

Eastwood, J. P., S. D. Bale, M. Maksimovic, I. Zouganelis, K. Goetz, M. L. Kaiser, and J.-L. Bougeret (2009), Measurements of stray antenna capacitance in the STEREO/WAVES instrument: Comparison of the radio frequency voltage spectrum with models of the galactic nonthermal continuum spectrum, *Radio Sci.*, *44*, RS4012, doi:10.1029/2009RS004146.

Hillan, D. S., I. H. Cairns, P. A. Robinson, and A. Mohamed (2010), Prediction of background levels for the Wind WAVES instrument and implications for the galactic background radiation, *J. Geophys. Res.*, *115*, A06102, doi:10.1029/2009JA014714.

Kraus, J. D., and R. J. Marhefka (2003), *Antennas for All Applications*, McGraw-Hill, New York.

Macher, W., T. H. Oswald, G. Fischer, and H. O. Rucker (2007), Rheometry of multi-port spaceborne antennas including mutual antenna capacitances and application to STEREO/WAVES, *Meas. Sci. Technol.*, *18*, 3731–3742.

Manning, R. E. (2000), Instrumentation for space-based low frequency radio astronomy, in *Radio Astonomy at Long Wavelenghts*, *Geophys. Monogr. Ser.*, vol. 119, edited by R. G. Stone et al., pp. 329–337, AGU, Washington, D. C.

Manning, R. E., and G. A. Dulk (2001), The galactic background radiation from 0.2 to 13.8 MHz, *Astron. Astrophys.*, *372*, 663–666.

Meyer-Vernet, N., and C. Perche (1989), Toolkit for antennae and thermal noise near the plasma frequency, *J. Geophys. Res.*, *94*, 2405–2415.

Meyer-Vernet, N., S. Hoang, K. Issautier, M. Moncuquet, and G. Marcos (2000), Plasma thermal noise: The long wavelength radio limit, in *Radio Astonomy at Long Wavelenghts*, *Geophys. Monogr. Ser.*, vol. 119, edited by R. G. Stone et al., pp. 67–74, AGU, Washington, D. C.

Novacco, J., and L. Brown (1978), Nonthermal galactic emission below 10 megahertz, *Astrophys. J.*, *221*, 114–123.

Nyquist, H. (1928), Thermal agitation of electric charge in conductors, *Phys. Rev.*, *32*, 110–113.

Schelkunoff, S. A., and H. T. Friis (1952), *Antennas: Theory and Practice*, John Wiley, New York.

Zarka, P., B. Cecconi, and W. S. Kurth (2004), Jupiter's low-frequency radio spectrum from Cassini/Radio and Plasma Wave Science (RPWS) absolute flux density measurements, *J. Geophys. Res.*, *109*, A09S15, doi:10.1029/2003JA010260.

Zouganelis, I., M. Maksimovic, N. Meyer-Vernet, S. D. Bale, J. P. Eastwood, A. Zaslavsky, M. Dekkali, K. Goetz, and M. L. Kaiser (2010), Measurements of stray antenna capacitance in the stereo/waves instrument: Comparison of the measured voltage spectrum with an antenna electron shot noise model, *Radio Sci.*, *45*, RS1005, doi:10.1029/2009RS004194.

S. D. Bale, Space Sciences Laboratory, University of California, Berkeley, CA 94720-7450, USA. (bale@ssl.berkeley.edu)

S. Hoang, M. Maksimovic, N. Meyer-Vernet, and A. Zaslavsky, Laboratoire d'Etudes Spatiales et d'Instrumentation en Astrophysique, Observatoire de Paris-CNRS-Université Pierre et Marie Curie-Université Denis Diderot, 5 place Jules Janssen, F-92195 Meudon, France. (sang.hoang@obspm.fr; milan.makismovic@obspm.fr; nicole.meyer@obspm.fr; arnaud.zaslavsky@obspm.fr)